2015 13th International Symposium on Modeling and Optimization in Mobile, Ad Hoc, and Wireless Networks (WiOpt)

Lifetime Optimization for Large-Scale Sink-Centric Wireless Sensor Networks

Soo-Hoon Moon
Dept. of Computer Science
Yonsei University, Seoul, Korea
nisti@yonsei.ac.kr

Seung-Jae Han
Dept. of Computer Science
Yonsei University, Seoul, Korea
seungjaehan@yonsei.ac.kr

***Abstract*—Energy efficiency is one of the most important issues of Wireless sensor networks (WSN) due to limited battery capacity. In sink-centric WSN (i.e., sensing data is collected by the sink node), this issue is particularly challenging due to the 'funnel effect' which means high energy consumption of the nodes near the sink. While clustering can be used to achieve scalability of WSN, previous works on energy optimal design of the cluster structure have limitations in the scalability. In this paper, we propose a scheme to build an energy optimal cluster structure for a sink-centric WSN. The most important finding of this paper is that energy optimality depends only the size of first three clusters from the sink node. Based on this finding, we design a very scalable clustering algorithm for optimal network lifetime. The algorithm is highly scalable since its time complexity is independent of the network size. We verify the correctness of the algorithm by comparing with the optimal results that are found by exhaustive search. Numerical evaluations are performed by modeling the off-the-shelf radio links such as IEEE 802.15.4 and IEEE 802.11.**

I. Introduction

Energy efficiency is one of the most critical issue of WSN with battery-powered sensor nodes. Extensive studies have been conducted to achieve energy efficiency from various viewpoints such as physical layer, MAC protocol, routing, cross-layer techniques, etc. A survey on these works is given in [1]. Recently, the advent of Internet of Things (IoT) boosts the demand of large-scale WSN [2], [3]. As the size of WSN increases, the energy efficiency becomes even more challenging because the radio transmission path is extended. For a large volume of small IoT devices, use of the cellular link is not always feasible due to high energy consumption and financial costs. Multi-hop communication using short-range radio is a more viable solution, in which sensing data generated by a sensor node is relayed by other sensor nodes to the sink node. The battery depletion of node in a route results in the interruption of data relaying, causing 'network partition' [4], [5].

Many WSN applications require periodic continuous data collection such as video sensing [6], environment tracking [7], [8], traffic surveillance [9]. In such applications, the traffic pattern is sink-centric. With sink-centric traffic, the network becomes more vulnerable to network partition since the energy consumption is concentrated near the sink node(s), which is called 'funnel effect'. This effect is intensified as the network size increases because the nodes near the sink must deal with more traffic than those far from the sink node. The energy consumption of the sensor nodes near the sink should be carefully optimized. Barring the straight-forward solution of provisioning large battery to the sensor nodes near the sink [10], clustering [11]–[13] has been considered as a solution for network scalability.

With clustering, adjacent sensor nodes are grouped into a cluster and a node is selected as the cluster head. Each sensor node forwards its data to the cluster head (i.e., intra-cluster data transmission) and the cluster head is responsible for the data delivery from that point. In some early WSN cluster schemes, direct transmission from each cluster to the sink was proposed but it is not feasible for large-scale WSN with low power sensor nodes. In typical WSN cluster schemes, data delivery to the sink is done by the forwarding of other cluster heads (i.e., inter-cluster data transmission). Inter-cluster data communication is a dominant factor in energy consumption since it involves longer distance transmission and larger amount of data than those of intra-cluster data communication. Thus, rotation of cluster head within a cluster is necessary. More importantly, unbalance in energy consumption among clusters can occur due to the difference of cluster size and the difference of the volume of relaying traffic. Battery exhaustion of a cluster will drop the overall routing efficiency by extending the routing paths (i.e., detouring). Eventually, some sensor traffic will not be delivered to the sink. We define the lifetime of a WSN as the duration until any sensor node loses its communication path to the sink node (i.e. network partition).

For maximizing the lifetime, it is important to balance the energy consumption of clusters. Note that the size of a cluster directly affects its energy consumption for both intra-cluster and inter-cluster transmission. It is because the cluster size decides the traffic volume of a cluster and the transmission distance between clusters. In particular, the size of near-sink clusters is important since they are the main victims of the funnel effect. In this paper, we propose a method to determine the size of clusters for optimal network lifetime. Optimal network lifetime means the longest possible duration until network partition. Subsequently, optimal cluster size means the size of cluster that results optimal network lifetime.

There exist previous works that study the network lifetime issue for sink-centric clustered WSN. For example, in [14] the lifetime of a cluster is probabilistically analyzed for a given sink-centric clustered WSN. This work does not address the issue of designing the optimal cluster structure. In [12] a clustering algorithm to relieve the funnel effect in sink-centric clustered WSN is proposed. It aims to extend the network lifetime by controlling the probability of each node becoming

978-3-9018-8273-9/15/ ©2015 IFIP

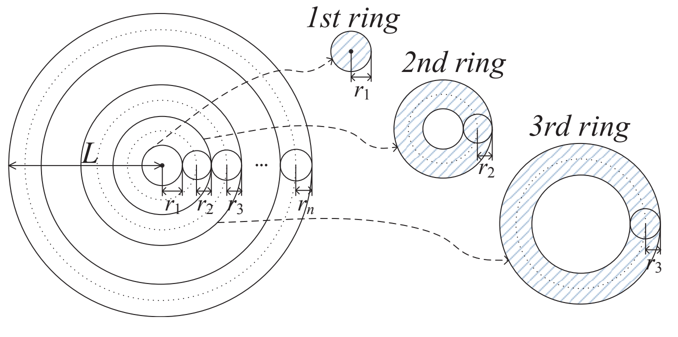

Fig. 1. Abstraction of a sink centric cluster structure

a cluster head during CH rotation. In essence, balancing the energy consumption of each cluster (region) is pursued, but the optimality is not guaranteed. Lastly, a scheme to decide the optimal cluster size for optimal lifetime is proposed in [15]. A key requirement of this scheme is that the number of clusters must to given. Obviously, knowing the optimal number of clusters is non-trivial. In contrast, our scheme derives both the number of clusters and the size of each cluster together.

The most important finding of this paper is that the network lifetime depends only the size of first three clusters from the sink node. Based on this finding, we design a very scalable clustering algorithm for optimal network lifetime. The time complexity of our scheme is independent of the network size. The main contributions of our paper are twofold:

1. We prove that the optimal network lifetime is dependent only on the size of first three clusters from the sink. In other words, the funnel effect can be analyzed by those three clusters.

2. We design an algorithm that computes the optimal cluster size. The algorithm is highly scalable since its time complexity is independent of the network size. We verify the correctness of the algorithm by comparing with the optimal results that are found by exhaustive search.

The rest of this paper is organized as follows. Section 2 describes the network model. Section 3 provides the formulation of energy consumption of clusters. Section 4 describes main theorem. Section 5 present our algorithm. A performance evaluation is presented in Section 6. Section 7 concludes the paper.

II. Network Model and Assumptions

We make some simplifying assumptions for the tractability of mathematical analysis. First of all, we consider a circular shape of network in which the sink node is at the center. Each cluster is also assumed to have a circular shape. Similar assumptions are made in other literature such as [15]. Sensor nodes are assumed to be uniformly distributed throughout the network with the density of Δ nodes per square meter. We assume each sensor node to periodically generate sensing data in the common rate of λ byte per second. We denote 'cycle' as the interval between two successive data generations.

We assume a cluster structure with doughnut-shaped rings as illustrated in Fig. 1. The inner-most ring with a single cluster in which the sink node is included is named '1st ring'. The radius of the cluster in the 1st ring is denoted by r_1. The sensor nodes outside the 1st ring form clusters that belong to the '2nd ring'. All the clusters in the 2nd ring have the same radius r_2. The neighboring clusters of the 2nd ring form the '3rd ring'. In this way, the entire network is covered with concentric cluster rings. Note that all clusters of the same ring have identical radius, but the clusters belonging to different rings may have different size.

The complexity of mathematical analysis is considerably reduced by adopting the cluster ring structure, as we need to determine only the size for each ring, instead of determining the size of each cluster. Since sensor nodes are uniformly distributed and the traffic generation rate is same for all sensors, the energy consumption pattern should be circular-symmetric in the optimal solution. Similar assumption is made in other literature like [15].

Within a cluster, all sensing data is forwarded to the cluster head. Then, the collected data is forwarded to the sink node via other cluster heads. We assume that inter-cluster data forwarding occurs only between the clusters of adjacent cluster rings. In other words, the data forwarding occurs from the $(i+1)$-th ring to the i-th ring. Similar assumption is adopted in [12]. We assume that the energy consumption of the sensor nodes in the same ring is balanced. This can be achieved by load balancing routing and cluster head rotation. Schemes such as [16], [17] may be used to this end. We exclude the energy consumption for intra-cluster data collection from the mathematical analysis, as the discrepancy in energy consumption by intra-cluster data collection is negligible in a large-scale WSN.

As stated earlier, we define the network lifetime as the duration until any sensor node loses its communication path to the sink, i.e. network partition. Since the energy consumption is balanced among the nodes in the same ring, our definition is equivalent to the duration until the batteries of all nodes in any ring have exhausted.

III. Formulation of Energy Consumption

In this section, we first formulate the energy consumption of each ring and then define the problem of network lifetime optimization.

A. Definitions regarding the Cluster Structure

Recall that the '1st ring' contains the sink node, and the $(i+1)$-th ring encircles the i-th ring. Let the number of rings in network be n. For $i = 1, \ldots, n$, let r_i be the radius of cluster in the i-th ring, briefly denoted by the i-th radius. $\boldsymbol{r} = \{r_1, \ldots, r_n\}$ represents the set of cluster sizes of the entire network. r_i has a value in the range of $[d_m, d_M]$. d_m and d_M are the minimum and the maximum transmission range respectively. Note that $\boldsymbol{r}$ uniquely represents a cluster ring structure.

The width of each ring is $2r_i$. The radius of outer rim of the i-th ring, $R_i = r_1 + 2\sum_{j=2}^{i} r_j$ $(1 \leq i \leq n,\ 1 \leq n)$, is the distance between the sink node to the outer edge of the i-th ring. When the i-th ring receives data, the transmission distance between two adjacent rings is $d_r(i) = r_i + r_{i+1}$ $(1 \leq i \leq n-1)$. We also define $d_s(i) = r_{i-1} + r_i$ $(i \geq 2)$ as the transmission distance when the i-th ring sends data. $d_r(n)$ and

$d_t(1)$ is zero since there is no data to deliver. Note that $d_r(i)$ and $d_t(i)$ cannot be greater than d_M(maximum transmission range). The area of each ring is $A(i) = \pi(R_i^2 - R_{i-1}^2)$ $(i \geq 2)$. $A(1)$ is equal to πr^2.

B. Energy Consumption Rate of a Ring

The energy consumption rate of a sensor node that belongs to the i-th ring ($E(i)$) is computed by the division of total energy consumption ($C(i)$) by the number of nodes in the ring ($N(i)$). $C(i)$ is the sum of energy consumption by sending and receiving data between rings. Recall that we ignore the energy consumption by intra-cluster data collection. The energy consumption by inter-cluster data transmission is computed by multiplying the amount of data and the per-bit energy consumption.

The i-th ring generates $\Delta\lambda A(i)$ of data. Recall that λ is the data generation rate. The i-th ring receives data from all of its outer rings, and sends those data plus its own generated data. We define $Q_r(i) = \Delta\lambda \sum_{j=i+1}^{n} A_j$ $(1 \leq i \leq n-1)$ and $Q_t(i) = \Delta\lambda \sum_{j=i}^{n} A_j$ $(i \geq 2)$ as the total amount of receiving and sending data for i-th ring, respectively. $Q_r(n)$ and $Q_t(0)$ is zero since there is no data to deliver. The per-bit energy consumption is the amount of energy needed to transmit or receive a single bit of data, which depends on the transmission distance. For the given transmission distance d, let $P_r(d)$ and $P_t(d)$ denote the per-bit energy consumption function when receiving and sending data, respectively. The path loss model should be integrated into these functions. In general, $P_r(d)$ and $P_t(d)$ are monotonically increasing functions.

Now, the total energy consumption of the i-th ring ($C(i)$) is defined as $C(i) = Q_r(i) \cdot P_r(d_r(i)) + Q_t(i) \cdot P_t(d_t(i))$. The number of nodes in the i-th ring ($N(i)$) is $\Delta A(i)$. We define $E(i; \boldsymbol{r})$ as the energy consumption rate of i-th ring in $\boldsymbol{r}$. Note that in computing $E(i)$, the node density Δ in $C(i)$ is eliminated by Δ in $N(i)$. This means that the energy consumption rate of each sensor node is independent of the node density Δ.

C. Problem Definition

The area that experiences the highest energy consumption by funnel effect will most rapidly exhaust its energy. Thus, the network lifetime is determined by this area. In our cluster ring structure, the unit of this area is a cluster ring since the energy consumption rate of nodes in same ring is identical. We define the most energy consuming area (MECA) as the ring that shows the highest energy consumption in the network. Note that multiple rings can be included in MECA. More specifically, we define $MECA(\boldsymbol{r})$ as a set of rings that are included in MECA for a given $\boldsymbol{r}$. We define $E_M(\boldsymbol{r}) = E(k)$ $(k \in \boldsymbol{r})$ as the energy consumption rate of the rings in $MECA(\boldsymbol{r})$. The radius of network (L) and per-bit energy consumption functions ($P_r(d)$, $P_t(d)$) are given. Therefore, when $\boldsymbol{r}$ is decided, $E_M(\boldsymbol{r})$ and $MECA(\boldsymbol{r})$ can be deterministically decided as follows:

$$E_M(\boldsymbol{r}) = \max_{i \in \mathbb{N}} E(i) \tag{1}$$

$$MECA(\boldsymbol{r}) = \arg\max_{i \in \mathbb{N}} E(i) \tag{2}$$

TABLE I. LIST OF NOTATIONS

Symbol	Description
r_i	Radius of cluster in the i-th ring $(meters)$
$\boldsymbol{r}$	Set of the cluster radii
R_i	Radius of the outer rim of the i-th ring
L	Radius of network
d	Transmission distance $(meters)$
$d_r(i), d_t(i)$	Transmission distance of the i-th ring (receiving, sending)
d_m, d_M	Minimum, maximum transmission range
$A(i)$	Area of the i-th ring (m^2)
$Q_r(i), Q_t(i)$	Amount of receiving, sending data of the i-th ring $(bytes)$
Δ	Node density $(nodes/m^2)$
λ	Data generation rate $(bits/sec \cdot node)$
q	Path loss exponent
$P_r(d), P_t(d)$	Per-bit energy consumption function (receiving, sending) (mW)
$C(i)$	Amount of total energy consumption of the i-th ring
$E(i)$	Average energy consumption rate of the i-th ring $(mW/node)$
$E(i; \boldsymbol{r})$	$E(i)$ for a set of cluster radii $\boldsymbol{r}$
MECA	Most energy consuming area
$MECA(\boldsymbol{r})$	Set of ring indexes of MECA for $\boldsymbol{r}$
$E_M(\boldsymbol{r})$	Energy consumption rate of MECA of $\boldsymbol{r}$
g	Granularity when searching optimal cluster radii
ω	Outermost ring in $MECA(\boldsymbol{r})$
$\boldsymbol{\omega}$	Set of consecutive rings of ω in $MECA(\boldsymbol{r})$
α	Innermost ring in $\boldsymbol{\omega}$
$\dot{\boldsymbol{r}}$	$\boldsymbol{r}$ that $r_{\alpha-1}$, r_α, $\ldots$, r_ω, $r_{\omega+1}$ are modified
$\ddot{\boldsymbol{r}}$	$\boldsymbol{r}$ in stable status: after iteration of $\boldsymbol{r}$-to-$\dot{\boldsymbol{r}}$ transition (Lemma 1)
$\boldsymbol{r}^*$	Set of optimal cluster radii
v	$(\omega+1)$-th ring of the most extended MECA (Section V-A)

The network lifetime is optimized when $E_M(\boldsymbol{r})$ is minimized. Thus, cluster size optimization problem is defined as follows:

$$\arg\min_{\boldsymbol{r}} \max_{i \in \mathbb{N}} E(i) \tag{3}$$

Equation (3) essentially finds $\boldsymbol{r}$ that maximizes the network lifetime. Let $\boldsymbol{r}^* = \{r_1^*, \ldots, r_n^*\}$ be an 'optimal' cluster radii set that is included in (3). Note that there can exist multiple sets of cluster radii ($\boldsymbol{r}^*$) that achieves optimal network lifetime. Table I summarizes notations used in this paper.

IV. KEY PROPERTY OF THE OPTIMAL NETWORK LIFETIME

A. Necessary Condition for the Optimality

In this section, we prove the following theorem which states the necessary condition that the optimal solution (i.e., the optimal cluster radii set) must possess.

Theorem 1: For $\forall \boldsymbol{r}^*$, $MECA(\boldsymbol{r}^*)$ includes the 1st ring or the 2nd ring. (i.e., $\arg\max_{i \in 1,2} E(i) \in MECA(\boldsymbol{r}^*)$)

By transposing this theorem into the sufficient condition for the non-optimality, theorem 1 means that if neither 1st or 2nd ring is included in $MECA(\boldsymbol{r})$, then $\boldsymbol{r}$ is not $\boldsymbol{r}^*$ (i.e., non-optimal). In other words, if $\boldsymbol{r}$ is optimal, there is no ring whose energy consumption rate exceeds the maximum of $E(1)$ and $E(2)$. Note that we only need r_1, r_2, and r_3 to calculate $E(1)$ and $E(2)$. This implies that finding the optimal solution is equivalent to finding an optimal set of $\{r_1, r_2, r_3\}$. We prove that theorem 1 in the remainder of this section.

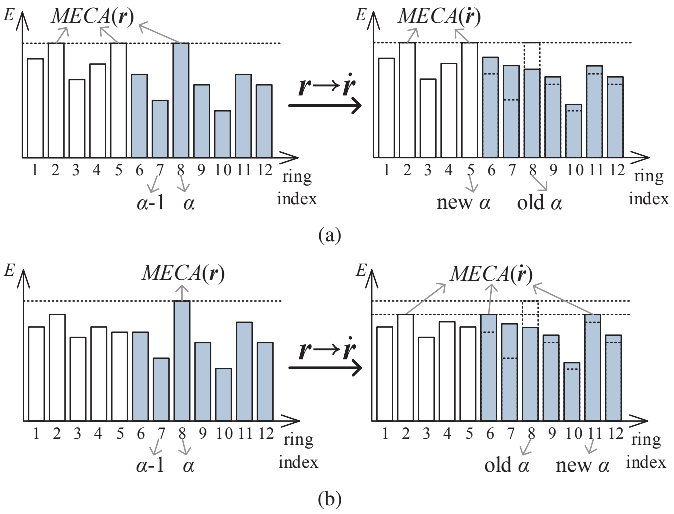

Fig. 2. Transition of the outermost ring of $MECA(\boldsymbol{r})$

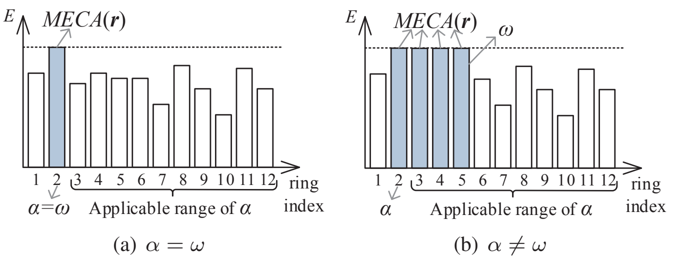

Fig. 3. Stable state after iterating $\boldsymbol{r}$-to-$\dot{\boldsymbol{r}}$ transition

B. Transition of Cluster Radii Set

To prove theorem 1, we start from the following intuition. If $E(i) < E(i+1)$ $(i \geq 1)$ for two adjacent i-th and $(i+1)$-th ring in $\boldsymbol{r}$, this relation can be reversed such as $E(i) \geq E(i+1)$ by adjusting some cluster radii in $\boldsymbol{r}$. We denote this action by 'job 1'. Now suppose that i-th ring is in MECA, and we try to perform job 1 while $E_M(\boldsymbol{r})$ (energy consumption rate of the rings in MECA) does not increase (which is denoted by 'job 2'). If it is possible to do job 2, MECA will be moved from the outer ring to the inner ring with equal or better network lifetime. We prove that it is always possible to do job 2 in lemma 1. By continuously applying job 2, MECA will eventually be moved to the center of the network, while its $E_M(\boldsymbol{r})$ does not increase.

Now let us introduce the notations used in lemma 1. Firstly, we denote by ω the outmost ring index in MECA. If the MECA includes other consecutive inner rings, we denote the set of those consecutive rings in MECA by $\boldsymbol{\omega}$. In particular, the innermost ring of $\boldsymbol{\omega}$ is denoted by α. Note that $\omega = \alpha$ if there is no consecutive ring of ω in MECA. Fig. 2 and Fig. 3 shows illustrative examples for α and ω. In Fig. 2(a), $MECA(\boldsymbol{r})$ includes the 2nd, 5th, and 8th ring, and the 8th ring is ω. The 8th ring has no consecutive inner rings in MECA, thus the 8th ring also becomes α. In Fig. 3(b), $MECA(\boldsymbol{r})$ includes the 2nd, 3rd, 4th, and 5th ring. The 5th ring is ω since it is the outmost ring in MECA. The 5th ring has consecutive inner rings in MECA that forms $\boldsymbol{\omega}$, and the 2nd ring is the innermost ring in $\boldsymbol{\omega}$. Thus, the 2nd ring becomes α.

Secondly, we denote by $\dot{\boldsymbol{r}}$ a cluster radii set which is the result of so-called $\boldsymbol{r}$-to-$\dot{\boldsymbol{r}}$ transition. This transition is applied to the rings from the $(\alpha-1)$-th ring to $(\omega+1)$-th ring. As a result, in $\dot{\boldsymbol{r}}$, the cluster radii of $\dot{r}_{,\alpha-1}$, $\dot{r}_{\alpha}$, ..., $\dot{r}_{\omega}$, $\dot{r}_{\omega+1}$ are modified. Note that for $\forall i \geq 2$, the change of r_i affects $E(k)$ for $\forall k \geq i-1$. This is because R_k for $\forall k \geq i$ is affected by the change of r_i and the equation for computing $E(k)$ for $\forall k \geq i$ includes R_k or r_i. Thus, by the change of $\boldsymbol{r}$ to $\dot{\boldsymbol{r}}$, all energy consumption rates from $(\alpha-2)$-th ring to the last ring (i.e., $E(\alpha-2), \ldots, E(n)$) are changed.

Lemma 1 ($\boldsymbol{r}$-to-$\dot{\boldsymbol{r}}$ transition): For $\forall \boldsymbol{r}$, let i be $\alpha \geq 3$ of $\boldsymbol{r}$. If $E(i-1;\boldsymbol{r}) < E(i;\boldsymbol{r})$, then there always exist $\dot{\boldsymbol{r}}$ such that $E(i;\boldsymbol{r}) > E(x;\dot{\boldsymbol{r}})$ for $\forall x \geq i$, and $E(i;\boldsymbol{r}) \geq E(y;\dot{\boldsymbol{r}})$ for $\forall y < i$.

Due to space limit, we omit the proof of Lemma 1, which is available in [18].

Lemma 1 means that if $(\alpha-1)$-th ring has lower energy consumption rate than that of α-th ring, we can make one of the inner ring of α-th ring be a new α of $MECA(\boldsymbol{r})$, or we can lower $E_M(\boldsymbol{r})$. Fig. 2 shows examples of applying lemma 1. In Fig. 2(a), α is moved to the inner ring since all $E(x;\dot{\boldsymbol{r}})$ for $\forall x \geq \alpha$ is less than $E(\alpha;\boldsymbol{r})$. If α-th ring is the only ring in $MECA(\boldsymbol{r})$ as in Fig. 2(b), the $\boldsymbol{r}$-to-$\dot{\boldsymbol{r}}$ transition lowers $MECA(\boldsymbol{r})$ to $MECA(\dot{\boldsymbol{r}})$ since $E(\alpha;\boldsymbol{r}) > E(\alpha;\dot{\boldsymbol{r}})$. The shaded bars are affected by $\boldsymbol{r}$-to-$\dot{\boldsymbol{r}}$ transition.

Based on Lemma 1, we can move the outmost ring of $MECA(\boldsymbol{r})$ toward the center of the network or we can reduce the average energy consumption of $MECA(\boldsymbol{r})$. If we continue applying $\boldsymbol{r}$-to-$\dot{\boldsymbol{r}}$ transition, the iteration stops when α becomes less than 3 as a condition of lemma 1. This means that $MECA(\boldsymbol{r})$ is placed in the center of network (i.e. the 1st and/or 2nd ring) after the iteration, and no more $\boldsymbol{r}$-to-$\dot{\boldsymbol{r}}$ transition is applicable. We call this status as 'stable state' of $\boldsymbol{r}$, which is denoted by $\ddot{\boldsymbol{r}}$. Fig. 3 shows examples of stable states. In both cases, $MECA(\boldsymbol{r})$ contains at least one of the 1st ring and 2nd ring.

If $\boldsymbol{r}$ is optimal (i.e., $\boldsymbol{r}^*$), $E_M(\boldsymbol{r}^*)$ (the optimal energy consumption rate) can not be lowered any further by $\boldsymbol{r}$-to-$\dot{\boldsymbol{r}}$ transitions. Via further $\boldsymbol{r}$-to-$\dot{\boldsymbol{r}}$ transitions, only the index of outmost ring (ω) in $MECA(\boldsymbol{r}^*)$ will be lowered, i.e., $MECA$ is moved toward the network center. We denote by $\ddot{\boldsymbol{r}}^*$ the stable state of $\boldsymbol{r}^*$.

By using lemma 1, we prove theorem 1 as follows.

Proof: Suppose that both of the 1st and 2nd ring are not included in $MECA(\boldsymbol{r}^*)$. Then, α must be equal to or greater than 3 during the iteration of $\boldsymbol{r}$-to-$\dot{\boldsymbol{r}}$ transition until getting the stable status ($\ddot{\boldsymbol{r}}^*$). However, the stop condition of iteration is $\alpha < 3$ and $\boldsymbol{r}$-to-$\dot{\boldsymbol{r}}$ transition is still applicable when $\alpha = 3$. This results in that α becomes less than 3, and violates the assumption (i.e., contradiction). Therefore, both of 1st and 2nd ring cannot be excluded in $MECA(\boldsymbol{r}^*)$, and at least one of them must be included in $MECA(\boldsymbol{r}^*)$. ■

The effect of theorem 1 is illustrated in Fig. 4 in which high energy consumption rate of the nodes around the sink node can be observed. The experiment setting is as follows. The network radius is 5000 meters. IEEE 802.11g link is used and the per-bit energy consumption function follows Equation (5). The path loss exponent is 2.6.

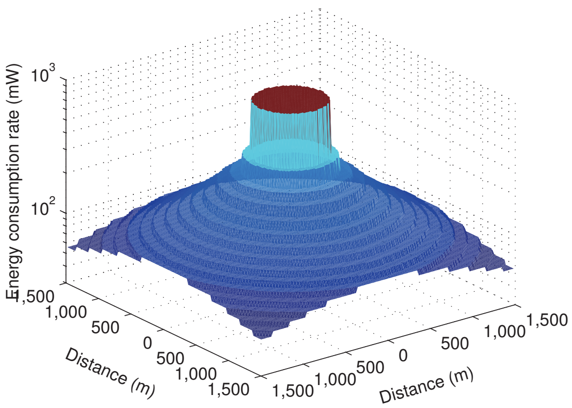

Fig. 4. Visual example of the energy consumption rate

$E_{max} \leftarrow \infty$ {Min. of $E_M(\boldsymbol{r})$ among all combinations)}
$\boldsymbol{r}^* \leftarrow \varnothing$
for all combinations of $\{r_1, r_2, r_3\}$ ($d_m < r_1 + r_2 < d_M$, $d_m < r_2 + r_3 < d_M$, granularity g) **do**
  calculate $E_M = \max(E(1), E(2))$ with $\{r_1, r_2, r_3\}$
  if $E_{max} > E_M$ **then**
    for $r_{v+1} (v \geq 3)$ **do**
      find r_{v+1} that satisfies Equation (4)
      $v \leftarrow v + 1$
    end for
  end if
  if $E(v) < E_M$ for $\exists r_{v+1} (d_m < r_{v+1} < d_M)$ **then**
    $E_{max} \leftarrow E_M$
    $\{r_1^*, r_2^*, \ldots, r_v^*\}$ in $r^* \leftarrow \{r_1, r_2, \ldots, r_v\}$
  end if
end for
return $v, \{r_1^*, r_2^*, \ldots, r_v^*\}$;

Fig. 5. Optimal cluster radii decision algorithm for r_i $(i \leq v)$.

V. Obtaining the Optimal Cluster Radii

A. Determining Cluster Radii within MECA

Thanks to theorem 1, the problem of finding $\boldsymbol{r}^*$ is significantly simplified. Theorem 1 ensures that if neither 1st or 2nd ring is included in $MECA(\boldsymbol{r})$, then $\boldsymbol{r}$ is not $\boldsymbol{r}^*$ (non-optimal). Note that none of r_1, r_2, and r_3 will be changed by $\boldsymbol{r}$-to-$\dot{\boldsymbol{r}}$ transition, if $\boldsymbol{r}$ is optimal (i.e., $\boldsymbol{r}^*$). In other words, to qualify as an optimal solution, $\boldsymbol{r}$ with a certain $\{r_1, r_2, r_3\}$ must be a stable state ($\ddot{\boldsymbol{r}}$).

We take an approach of exhaustive search to find the optimal set of $\{r_1, r_2, r_3\}$. Our method checks the validity of $\{r_1, r_2, r_3\}$ as a valid candidate of an optimal solution as follows. At first, we assume that the set of $\{r_1, r_2, r_3\}$ is a $\ddot{\boldsymbol{r}}$. We check if the 2nd ring is in MECA, and if true, we try to 'extend' the MECA as far as possible for this set of $\{r_1, r_2, r_3\}$. The extension of MECA is conducted by sequentially finding r_4 and further cluster radii that makes the 3rd ring and further rings have same energy consumption rates as that of rings in MECA. When no more extension is possible, we call this status as 'the most extended MECA'. We denote by v as the adjacent outer ring of the most extended MECA. The cluster radii set of $\{r_1, \ldots, r_v\} (v \geq 3)$ is composed after the extension of MECA. If the assumption is true, the v-th ring will have lower energy consumption rate than that of MECA, i.e. $E(v) < E_M(\boldsymbol{r})$.

Fig. 5 shows the pseudo code of our optimal cluster radii decision algorithm for the rings r_i $(i \leq v)$. We generate all possible combinations of r_1, r_2, and r_3 that do not exceed the distance limit of transmission. Then, we calculate $E(1)$ and $E(2)$ for each set of cluster radii $\{r_1, r_2, r_3\}$. The greater one between $E(1)$ and $E(2)$ becomes the energy consumption rate of the rings in MECA. We denote E_M as $\max(E(1), E(2))$. Note that E_M is equal to $E_M(\boldsymbol{r})$ since the 1st ring or 2nd ring is always included in $MECA(\boldsymbol{r})$. Now, we extend $MECA(\boldsymbol{r})$ as far as possible. Recall that v is an adjacent outer ring of the outermost ring in the most extended $MECA(\boldsymbol{r})$. v $(v \geq 3)$ is currently unknown since the most extended MECA is not decided. Recall that r_1, ..., r_v, and r_{v+1} are needed to calculate $E(v)$. If we know all r_j $(j \leq v)$ and $E(v-1) = E(v)$, then r_{v+1} can be deterministically calculated. We first calculate r_4 that satisfies $E_M = E(3)$, and then sequentially calculate r_{v+1} that satisfies $E_M = E(v-1) = E(v)$ for $\forall v \geq 3$. If r_{v+1} is successfully calculated, the v-th ring becomes a member of MECA. The condition of r_{v+1} is as follows:

$$r_{v+1} = P_r^{-1}(X_v) - r_v \tag{4}$$

P_r^{-1} is an inverse function of the per-bit energy consumption function for receiving data (P_r). The derivation process of (4) is described in [18]. We omit the explanation due to the space limit.

We iteratively find the next cluster radius using (4) until no applicable r_{v+1} is found, which satisfies the condition of $E(v) = E_M$ and the distance limit of transmission $[d_m, d_M]$ is not violated. When the iteration ends, we have the cluster radii of $\{r_1, r_2, \ldots, r_v\}$. The $(v-1)$-th ring is the outmost ring of the most extended MECA.

If this MECA is valid (i.e. the set of $\{r_1, r_2, r_3\}$ is the elements of $\ddot{\boldsymbol{r}}$), the adjacent outer ring of MECA should have lower energy consumption rate than that of MECA. We search r_{v+1} that holds this condition, i.e. $E(v) < E_M$. If there exists such r_{v+1}, we compare E_M with the best ever found E_M, denoted as E_m which has minimum of E_M ever found during this search. If current E_M is better (i.e. smaller) than E_m, we save the current E_M as a new E_m with current cluster radii set $\{r_1, r_2, \ldots, r_v\}$. On the other hand, if there exists no applicable r_{v+1} that holds the condition, this set of $\{r_1, r_2, r_3\}$ is disqualified and we move on to the next combination of $\{r_1, r_2, r_3\}$. By iterating this process for all combinations of r_1, r_2, and r_3, we can derive a best E_M with the optimal cluster radii of the rings in MECA.

B. Determining Cluster Radii outside MECA

The cluster radii from r_1 to r_v is decided by the algorithm of Fig. 5, and now we decide the rest of cluster radii from r_{v+1} to the outermost cluster radius. Unlike the cluster radii within MECA, the optimal solution for the rest of cluster radii is not unique. In other words, there exists multiple r_i $(i > v)$ that $E(i-1)$ does not exceed E_M.

We only need a particular value of cluster radii among all feasible r_i. We start from the decision of r_{v+1}. We select an

$c_r \leftarrow d_M/4$ {constant for identical size of radius}
for $i = v+1, v+2, \dots$ **do**
  $r_i \leftarrow c_r$, $r_{i+1} \leftarrow c_r$, $r_{i+2} \leftarrow c_r$
  calculate $E(i-1), E(i), E(i+1)$ with $\{r_1, \dots, r_{i+2}\}$
  if $\max(E(i-1), E(i), E(i+1)) \leq E_M$ **then**
    set all $r_j^*(j \geq i)$ in $\boldsymbol{r}^*$ as c_r;
    return $\boldsymbol{r}^*$
  end if
  for $r_i = d_M - r_{i-1}, d_M - r_{i-1} - g, \dots, d_m$ **do**
    if $E(i-1) \leq E_M$ **then**
      $r_i^* \leftarrow r_i$
      exit this for
    end if
  end for
end for

Fig. 6. Optimal cluster radii decision algorithm for r_i $(i > v)$.

initial value of r_{v+1} as $(d_M - r_{i-1})$, which is the maximum value of r_{v+1}. With that r_{v+1}, we calculate $E(i-1)$ and compare it with E_M to identify that r_{v+1} is feasible. If $E(i-1)$ does not exceed E_M, we select that r_{v+1} as an optimal r_{v+1} and move on to the search of r_{v+2}. This process is continued until all cluster radii are decided.

To reduce the time complexity for the decision process, we utilize the following property of $E(i)$. If the derivative of $E(i)$ with respect to i is negative from a certain i, we set all the rest of cluster radii to an identical value. At that stage, if $E(i)$ does not exceed d_M, we set the rest of cluster radii to that value. The algorithm to decide the cluster radii r_i $(i > v)$ is described in Fig. 6. The complexity of the algorithm in Fig. 6 is $O(MN)$. M is the number of the rest of cluster radii, and N is the number of values that a cluster radius can have. The algorithm iterates M times if appropriate identical size is not found in worst case. It takes $O(N)$ to decide each cluster radius.

VI. Evaluations

A. Evaluation Settings

In this section, we verify the optimality of our solution. To this end, we compare the results of the proposed methods with the optimal solution that are obtained by exhaustively search for all possible cluster configurations in a brute force manner.

Two common wireless link technologies, IEEE 802.11g and IEEE 802.15.4, are considered. We utilize the experimental measurement data of these radio interfaces to decide the parameters of per-bit energy consumption function. We have fitted the measurement data of [19], [20] for IEEE 802.11g and [21] for IEEE 802.15.4 to the polynomial equations. The following is the resulting per-bit energy consumption function, where d is the transmission distance.

$$P(d) = 45 + 1.786 \cdot 10^{-3} \cdot d^{2.6} \tag{5}$$

$$P(d) = 103.54 + 4.8256 \cdot d^{1.0} \tag{6}$$

Equation (5) is for IEEE 802.11g and Equation (6) is for IEEE 802.15.4. We use $P(d)$ for $P_t(d)$ and $P_r(d)$, i.e. $P(d) = P_t(d) = P_r(d)$. The path loss exponent q is 2.6 for both Equations (5) and (6).

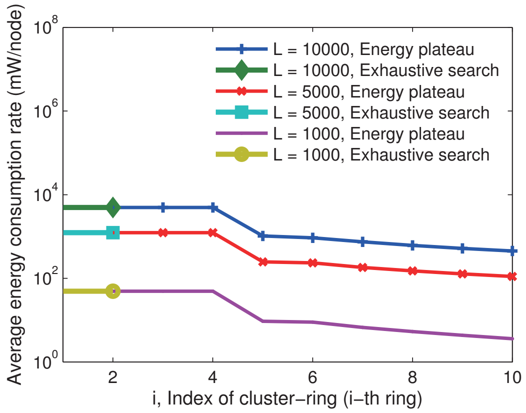

Fig. 7. $E(i)$ by network size (L) with IEEE 802.11g $(q = 2.6)$

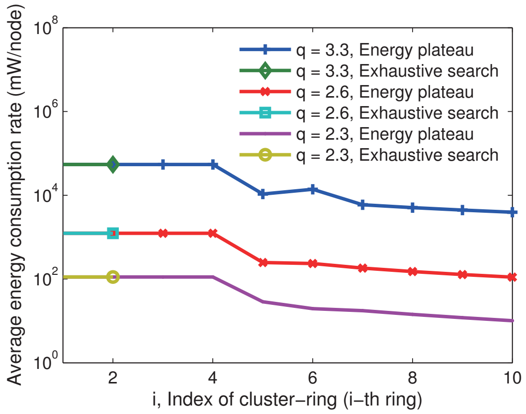

Fig. 8. $E(i)$ by path loss exponent (q) with IEEE 802.11g $(L = 5000\text{m})$

For IEEE 802.11g link, Equation (5) is yielded by fitting the following data: the 14 dBm of transmission power, 1320 mW of energy consumption on radio interface, $\{-68, -72, -78, -82, -86, -88, -89, -90\}$ dBm of receiving threshold for $\{27, 24, 18, 12, 9, 6, 4.5, 3\}$ Mbps of transmission speed, respectively. The receiving antenna gain is 1 dBi. The energy consumption is constant regardless of the transmission speed for IEEE 802.11g. The transmission distance is determined by the path loss exponent. We vary the path loss exponent q to simulate the various path loss environments. $P(d) = 45 + 4.464 \cdot 10^{-4} \cdot d^{2.3}$ when $q = 2.3$, and $P(d) = 45 + 4.545 \cdot 10^{-2} \cdot d^{3.3}$ when $q = 3.3$.

For IEEE 802.15.4 link, Equation (6) is the fitted function from the following data: $\{0, -1, -3, -5, -7, -10, -15, -25\}$ dBm of transmission power for $\{30.7, 28.4, 22.1, 21.9, 19.6, 17.5, 15.2\}$ mW of energy consumption, respectively. The transmission speed is 0.122 Mbps with -90 dBm of the receiving threshold. The receiving antenna gain is 0 dBi. IEEE 802.15.4 controls its transmission power according to the transmission distance. Equation (6) is the resulting power consumption that both the power control of module and the path loss is considered. The transmission distance is determined by the path loss exponent q. $P(d) = 103.54 + 4.8256 \cdot d^{0.88}$ when $q = 2.3$, and $P(d) = 103.54 + 4.8256 \cdot d^{1.26}$ when $q = 3.3$.

In the exhaustive search, the radii sets for all possible combinations of $\{r_1, r_2, r_3, \dots, r_n\}$ are checked. To avoid

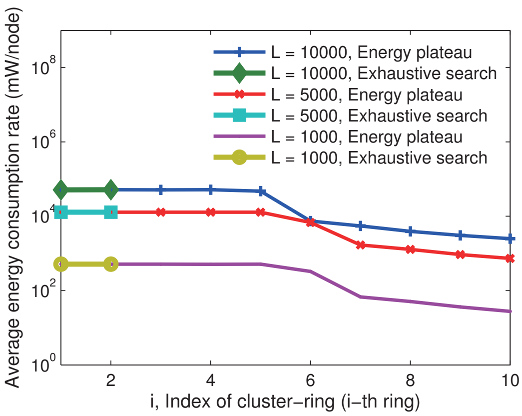

Fig. 9. $E(i)$ by network size (L) with IEEE 802.15.4 ($q = 2.6$)

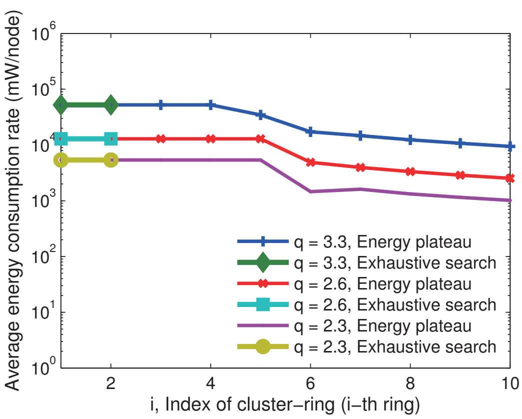

Fig. 10. $E(i)$ by path loss exponent (q) with IEEE 802.15.4 ($L = 5000$m)

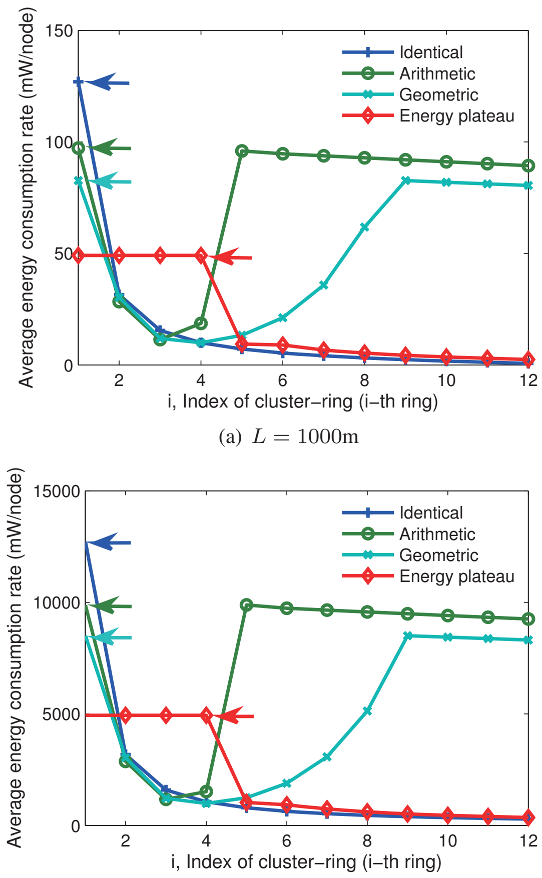

(a) $L = 1000$m

(b) $L = 10000$m

Fig. 11. $E(i)$ by cluster radii decision strategy with IEEE 802.11g ($q = 2.6$)

prohibitively high computation time, we reduce the number of combinations as follows. We gradually increase the number of variables from $\{r_1, r_2, r_3, r_4\}$ to $\{r_1, r_2, r_3, \ldots, r_k\}$ $(k \geq 4)$ while r_k is used for the rest of rings. If the result does not change even if the number of variables is increased, we stop the search. Since there exists a limit on transmission range, we check the cluster radius from d_m to d_M with the granularity g. Throughout this section, we use the granularity of $g = 0.01$ meter. The node density Δ is 1 node/m^2, and each node generates 1K bytes of data per cycle. Our scheme is named as "Energy plateau" while the exhaustive search scheme is named as "Exhaustive".

B. Verification of Optimality

1) Network Size: We first vary the size of the network (L). We calculate the energy consumption rate $E(i)$ of each ring i for various cases, which are plotted in Fig. 7. The unit of L is meters. IEEE 802.11g is used for the link, and the path loss exponent q is set to 2.6. For the exhaustive search method, we show $E(i)$ of the first two rings ($E(1)$ and $E(2)$) with thick lines, since multiple optimal radii set only shares the size of the 1st and 2nd ring as the highest energy consumption rates. For the proposed method, the energy consumption rates of the first ten cluster rings are plotted with thin lines in Fig. 7. For all sizes of network, the maximum energy consumption rate of both methods match exactly. Other observations are as follows. $E(i)$ of the rings in MECA shows same energy consumption rate while $E(i)$ outside of MECA does not exceed the maximum energy consumption rate. The result verifies theorem 1.

2) Path Loss Exponent: Now, we vary the path loss exponent. In Fig. 8, we compare the results of our method with the optimal solution for various path loss exponents. We can observe exact match between the results of our method and optimal solution for all cases of path loss exponent. IEEE 802.11g is used as the link technology, and the network radius is 5000 meters. As the path loss exponent q increases, the optimal size of clusters decreases, as expected. The proposed algorithm properly works in various path loss environments.

3) Radio Interface: We have verified the optimality of the proposed method by using IEEE 802.15.4 link. Fig. 9 show the results for various network sizes. Fig. 10 show the results for various path loss exponents. The general trends are the same as the case of IEEE 802.11g. As the case of IEEE 802.11g, the proposed method generates optimal solution in various sizes of network and path loss environment.

C. Comparison with Heuristics

Next, we compare the energy efficiency of the results of the proposed method with some heuristic strategies. We use three heuristic strategies: 'Identical', 'Arithmetic', and 'Geometric'. 'Identical' sets all radii as the same value, i.e. r_i $(i \geq 1) = r$. 'Arithmetic' imitates an arithmetic progression. r_1 is set to the

TABLE II. BEST PARAMETERS BY THE STRATEGIES

Strategy	$L = 1000m$	$L = 10000m$
Identical	$r = 39.27$	$r = 39.17$
Arithmetic	$c = 65.9, a = -19.9$	$c = 65.1, a = -19.0$
Geometric	$c = 70.9, a = 0.57$	$c = 69.8, a = 0.59$

initial term c, and the next cluster radius is decided by adding a common difference a, i.e. $r_1 = c,\ r_{i+1} = r_i + a$. 'Geometric' is imitating a geometric progression. The next cluster radius is decided by multiplying a common ratio a, i.e. $r_1 = c,\ r_{i+1} = r_i \cdot a$.

Fig. 11 compares the performance of the three strategies with the proposed method. We show only the IEEE 802.11g results. For the comparison, we have searched the best variables that maximizes the network lifetime for each heuristic strategy. Table II summarized the best parameters by the strategies. In all cases, the proposed method clearly outperforms the best case of each heuristic strategy. Recall that the lower the maximum of the average energy consumption rate is, the longer the network lifetime becomes.

More specifically, in Table II, the optimal parameter of a for Arithmetic is negative, and that of a for Geometric is less than 1. These mean that the optimal cluster size gradually decreases as the ring index increases. The reason is as follows. Due to the nature of the sink-centric traffic, the center of the network tends to become the critical area that decides the network lifetime. If the network is large, the amount of data to forward is not much different between the rings in the critical area. Therefore, the important factor is the number of nodes that share the forwarding burden and the distance between the clusters. The inner ring needs to have larger radius than the outer ring so that more nodes share the energy consumption burden.

VII. CONCLUSION

In this paper, we have presented a method to compute the optimal cluster sizes for maximizing the network lifetime of large-scale sink-centric clustered WSNs. The key contribution of our paper is to mathematically prove that the 1st and/or 2nd ring is always the most energy consuming points. This property is utilized to devise a scalable algorithm that produces a cluster structure for optimal network lifetime. Though our algorithm is designed with certain assumptions which may not always hold in practice, it can provide good approximation even in case such assumptions are not applicable.

ACKNOWLEDGMENT

This work was supported by the National Research Foundation of Korea(NRF) grant funded by the Korea government(MSIP) (No. 2013R1A2A2A01068325).

REFERENCES

[1] G. Anastasi, M. Conti, M. Di Francesco, and A. Passarella, "Energy conservation in wireless sensor networks: A survey," *Ad Hoc Networks*, vol. 7, no. 3, pp. 537–568, 2009.

[2] M. Ma and Y. Yang, "Sencar: an energy-efficient data gathering mechanism for large-scale multihop sensor networks," *Parallel and Distributed Systems, IEEE Transactions on*, vol. 18, no. 10, pp. 1476–1488, 2007.

[3] R. N. Murty, G. Mainland, I. Rose, A. R. Chowdhury, A. Gosain, J. Bers, and M. Welsh, "Citysense: An urban-scale wireless sensor network and testbed," in *Technologies for Homeland Security, 2008 IEEE Conference on*. IEEE, 2008, pp. 583–588.

[4] K. Akkaya, F. Senel, A. Thimmapuram, and S. Uludag, "Distributed recovery from network partitioning in movable sensor/actor networks via controlled mobility," *Computers, IEEE Transactions on*, vol. 59, no. 2, pp. 258–271, 2010.

[5] Y. K. Joshi and M. Younis, "Autonomous recovery from multi-node failure in wireless sensor network," in *Global Communications Conference (GLOBECOM), 2012 IEEE*. IEEE, 2012, pp. 652–657.

[6] V. Jelicic, M. Magno, D. Brunelli, G. Paci, and L. Benini, "Context-adaptive multimodal wireless sensor network for energy-efficient gas monitoring," *Sensors Journal, IEEE*, vol. 13, no. 1, pp. 328–338, 2013.

[7] S. Manna, S. S. Bhunia, and N. Mukherjee, "Vehicular pollution monitoring using iot," in *Recent Advances and Innovations in Engineering (ICRAIE), 2014*. IEEE, 2014, pp. 1–5.

[8] S. E. Díaz, J. C. Pérez, A. C. Mateos, M.-C. Marinescu, and B. B. Guerra, "A novel methodology for the monitoring of the agricultural production process based on wireless sensor networks," *Computers and Electronics in Agriculture*, vol. 76, no. 2, pp. 252–265, 2011.

[9] J. A. Rodríguez-Serrano and S. Singh, "Trajectory clustering in cctv traffic videos using probability product kernels with hidden markov models," *Pattern Analysis and Applications*, vol. 15, no. 4, pp. 415–426, 2012.

[10] S. Chen, P. Sinha, N. B. Shroff, and C. Joo, "Finite-horizon energy allocation and routing scheme in rechargeable sensor networks," in *INFOCOM, 2011 Proceedings IEEE*. IEEE, 2011, pp. 2273–2281.

[11] X. Zhu, J. Li, Y. Xia, X. Gao, and G. Chen, "An efficient distributed node clustering protocol for high dimensional large-scale wireless sensor networks," in *Proceedings of the 8th International Conference on Ubiquitous Information Management and Communication*. ACM, 2014, p. 4.

[12] D. Wei, Y. Jin, S. Vural, K. Moessner, and R. Tafazolli, "An energy-efficient clustering solution for wireless sensor networks," *Wireless Communications, IEEE Transactions on*, vol. 10, no. 11, pp. 3973–3983, 2011.

[13] H. Taheri, P. Neamatollahi, O. M. Younis, S. Naghibzadeh, and M. H. Yaghmaee, "An energy-aware distributed clustering protocol in wireless sensor networks using fuzzy logic," *Ad Hoc Networks*, vol. 10, no. 7, pp. 1469–1481, 2012.

[14] M. Noori and M. Ardakani, "Lifetime analysis of random event-driven clustered wireless sensor networks," *Mobile Computing, IEEE Transactions on*, vol. 10, no. 10, pp. 1448–1458, 2011.

[15] T. Shu and M. Krunz, "Coverage-time optimization for clustered wireless sensor networks: a power-balancing approach," *IEEE/ACM Transactions on Networking (TON)*, vol. 18, no. 1, pp. 202–215, 2010.

[16] C. Petrioli, M. Nati, P. Casari, M. Zorzi, and S. Basagni, "Alba-r: load-balancing geographic routing around connectivity holes in wireless sensor networks," *Parallel and Distributed Systems, IEEE Transactions on*, vol. 25, no. 3, pp. 529–539, 2014.

[17] S. Soro and W. B. Heinzelman, "Cluster head election techniques for coverage preservation in wireless sensor networks," *Ad Hoc Networks*, vol. 7, no. 5, pp. 955–972, 2009.

[18] S.-H. Moon and S.-J. Han. (2015) Appendix for lifetime optimization for large-scale sink-centric clustered wireless sensor networks. Extended Version. [Online]. Available: https://www.dropbox.com/sh/fbuypvyj1aogwnk/AADY3zBXHyJKLbUoG0gDFjQza?dl=0

[19] D. McIntire, K. Ho, B. Yip, A. Singh, W. Wu, and W. J. Kaiser, "The low power energy aware processing (leap) embedded networked sensor system," in *Proceedings of the 5th international conference on Information processing in sensor networks*. ACM, 2006, pp. 449–457.

[20] Texas Instruments. (2003) Low power advantage of 802.11a/g vs. 802.11b. White Paper. [Online]. Available: http://focus.ti.com/pdfs/bcg/80211_wp_lowpower.pdf

[21] B. Bougard, F. Catthoor, D. C. Daly, A. Chandrakasan, and W. Dehaene, "Energy efficiency of the ieee 802.15. 4 standard in dense wireless microsensor networks: Modeling and improvement perspectives," in *Design, Automation, and Test in Europe*. Springer, 2008, pp. 221–234.